Complex Formation between Anisole and Boron Trifluoride: Structural and Binding Properties

Tao Lin,[†,‡] Weijiang Zhang,[†] and Lichang Wang*[,‡]

School of Chemical Engineering and Technology, Tianjin University, Tianjin 300072, China, and Department of Chemistry and Biochemistry, Southern Illinois University, Carbondale, Illinois 62901

Received: June 30, 2008; Revised Manuscript Received: September 16, 2008

The structures, energetics, and binding characteristics of complexes formed between anisole ($C_6H_5OCH_3$) and boron trifluoride (BF_3) were investigated using MP2 and B3LYP methods with 6-31+G(d,p) and 6-311+G(d,p) basis sets. Among the complexes with a 1:1 ratio of $C_6H_5OCH_3$ to BF_3, both B3LYP and MP2 methods predict the same structures and relative stability of the isomers; however, the B3LYP binding energies are smaller than the MP2 energies. Furthermore, the weaker the interaction, the greater the discrepancy in binding energy. The charge decomposition analysis (CDA) showed that there are two types of complexes: the Lewis acid−base adduct and the van der Waals complexes. The CDA results also illustrated that there is a significant donation from the oxygen lone pair electrons to the boron vacant orbital in the adduct. The van der Waals complexes were formed through the aromatic ring and BF_3 interaction or through the H and F interactions. The MP2 results showed that the formation of adduct at room temperature is thermodynamically favorable. Among the 1:2 $C_6H_5OCH_3-BF_3$ complexes, the most stable structure consists of both the Lewis acid−base and van der Waals binding; i.e., one BF_3 binds with $C_6H_5OCH_3$ to form $C_6H_5OCH_3 \cdot BF_3$ adduct, while the other BF_3 binds with this adduct through van der Waals interactions. The calculated binding energy of the 1:1 complex is close to the experimental heat of formation, which suggests that the 1:1 complexes are the most likely species in the $C_6H_5OCH_3$ and BF_3 mixture.

1. Introduction

Boron compounds have been used in many applications. For instance, boron hydrides have recently been studied as potential hydrogen storage materials.[1−3] Boron trifluoride (BF_3), on the other hand, has been used as catalysts in photochemical reactions[4] and in the separation of boron isotopes.[5−9] In the chemical exchange process of separating ^{10}B from ^{11}B, anisole (methylphenyl ether, $C_6H_5OCH_3$) is so far the best complexation agent because the use of anisole allows the exchange column, where the chemical exchange process takes place, to be operated at room temperature and ambient pressure.[5−7] Complex formation between anisole and boron trifluoride is the first and also an important step of the exchange reactions, but it has not been investigated extensively.[5,10] The heat released from the $C_6H_5OCH_3$ and BF_3 complex formation was measured to be 12.1 kcal/mol.[5] There was also an infrared study on the $C_6H_5OCH_3$ and BF_3 complex with a 1:1 ratio.[10] To further optimize operation conditions or to search for better complexation agents for the chemical exchange process, it is crucial to understand the binding nature of the $C_6H_5OCH_3$ and BF_3 complexes. Are the complexes formed as the Lewis acid−base adducts or as van der Waals complexes? Furthermore, the existence of complexes containing more than one BF_3 molecule was reported in the other ether−BF_3 complexes.[11] Therefore, it is also important to study the ratio of anisole to boron trifluoride in the complexes.

Providing answers to these questions is the main focus of this research. As such, we performed the second-order Møller−Plesset (MP2) and density functional theory (DFT) calculations on the $C_6H_5OCH_3-BF_3$ complexes using both 6-31+G(d,p) and 6-311+G(d,p) basis sets. Specifically, we calculated the structures and binding energies of $C_6H_5OCH_3-BF_3$ 1:1 and 1:2 complexes. To understand the binding characteristics of these complexes, we also did charge decomposition analysis. Moreover, our choice of different methods and basis sets is to further assess the accuracy of the method/basis set in the description of weak interactions.

Although studies of $C_6H_5OCH_3$ and BF_3 complexes are largely lacking, there are many experimental and theoretical studies devoted to the formation of BF_3 complexes with other molecules.[5,12−39] These include studies of BF_3 complexes with molecules involving nitrogen atoms (such as with NH_3,[25−29] HCN,[27,32,33] and C_5H_5N[34]), oxygen atoms,[5,24,35−37] sulfur atoms,[38,39] fluorine atoms,[17,18] or benzene rings.[16] Because anisole consists of two distinguished parts, a benzene ring and a methoxy group, the studies of BF_3 complexes with molecules such as those mentioned above can provide useful information to the current work and also allow us to make comparisons. Saenz et al. reported the structures, vibrational frequencies, and relative energies on the complexes of BF_3 with diethyl ether, dimethyl ether, and methanol.[24] Their results show that the complexes bind through the B and O interaction. For the $(CH_3CH_2)_2O-BF_3$ complexes, the binding energy is −13.5 kcal/mol and the B−O distance is 1.642 Å, which were obtained using MP2/6-311++G(3df,2pd) with the basis set superposition error (BSSE) and zero point energy (ZPE) corrections for energy. Similarly, for the $(CH_3)_2O-BF_3$ complexes, the calculated binding energy is −13.1 kcal/mol and the B−O distance is 1.671 Å. As for the CH_3OH-BF_3 complexes, the binding energy is −11.0 kcal/mol and the B−O distance is 1.687 Å. These three sets of data show a strong correlation between the B−O distance and binding

* To whom correspondence should be addressed. E-mail: lwang@chem.siu.edu. Telephone: (618) 453-6476.
† Tianjin University.
‡ Southern Illinois University.

10.1021/jp805748b CCC: $40.75 © 2008 American Chemical Society
Published on Web 12/04/2008

energy: a stronger binding corresponds to a shorter B−O distance. Tarakeshwar et al. reported that the binding energy of benzene and BF_3 is −3.29 kcal/mol, which was obtained using MP2/6-311++G(3df, 2p) method including the BSSE and ZPE corrections.[16] It was found that the BF_3 molecule prefers to lie directly above one of the benzene carbons; therefore it interacts with the π electron cloud of the benzene ring. Comparison in binding energies of the above BF_3 complexes demonstrates clearly that there is a much stronger interaction between the BF_3 and O atom than the BF_3 and benzene ring.

Studies of complex formation with a 1:1 ratio of anisole to ammonia[25,40] and to water[22,23] were also carried out. For the anisole−ammonia complexes, it was found that the most stable structure is through the π ring···H interaction,[40] while, for the anisole−water complexes, the most significant contribution to the binding is through the interaction between the O atom of anisole and the σ HO bond of water.[22] It is worth mentioning that, in these anisole containing complexes, either anisole−ammonia or anisole−water, the OC bond of the methoxy group is still in the same plane as the benzene ring. However, as our results have shown, which will be described in section 3, it is not the case when anisole forms a complex with BF_3.

2. Computational Details

In this work, we studied the complex formation between anisole and boron trifluorides,

$$C_6H_5OCH_3 + nBF_3 \rightarrow C_6H_5OCH_3 - n(BF_3) \qquad (1)$$

where n is the number of BF_3 in the complex.

Ab initio and density functional theory (DFT) calculations were performed for the above reaction using Gaussian03.[41] Specifically, the MP2 theory[42,43] and the Becke's three-parameter exchange functional with the Lee−Yang−Parr correlation functional (B3LYP)[44−47] were used. Both 6-31+G(d,p) and 6-311+G(d,p) basis sets were used in the calculations. Full geometry relaxations were performed without any constraints. In the case in which a symmetry constraint was enforced, the results will be explicitly stated in the discussion below. The SCF convergence was 10^{-8} au. The gradient and energy convergence was 10^{-4} and 10^{-5} au, respectively. Frequency calculations were performed on all the structures reported here to ensure that these structures are indeed the minima. All the frequencies can be found in the Supporting Information.

In addition to the structural parameters, i.e., bond distance, bond angle, and dihedral angle, we also calculated the binding energy, formation enthalpy, and Gibbs free energy change for reaction 1 as follows. The binding energy, ΔE, was calculated by

$$\Delta E = E(\text{complex}) - E(C_6H_5OCH_3) - nE(BF_3) \qquad (2)$$

where E(complex), $E(C_6H_5OCH_3)$, and $E(BF_3)$ are the energies of the complex, $C_6H_5OCH_3$, and BF_3, respectively. The number of BF_3 monomers in the complex is denoted by n, which is 1 or 2 in this study. The binding energies were also calculated by correcting for the BSSE using the counterpoise method of Boys and Bernardi.[48] Since the present study dealt with weak interactions, we employed a 50% BSSE correction strategy, which was used by other researchers dealing with the systems of similar weak interactions.[22,49−56] The binding energies with inclusion of both the 50% BSSE and ZPE corrections, ΔE_0, were also calculated.

The formation enthalpy of reaction (1) at 298 K and ambient pressure, ΔH, was given by

$$\Delta H = H(\text{complex}) - H(C_6H_5OCH_3) - nH(BF_3) \qquad (3)$$

where H(complex), $H(C_6H_5OCH_3)$, and $H(BF_3)$ are the enthalpies of the complex, $C_6H_5OCH_3$, and BF_3 at 298 K and ambient pressure, respectively. Similarly, the Gibbs free energy change of reaction 1 at 298 K and ambient pressure, ΔG, was calculated using

$$\Delta G = G(\text{complex}) - G(C_6H_5OCH_3) - nG(BF_3) \qquad (4)$$

where G(complex), $G(C_6H_5OCH_3)$, and $G(BF_3)$ are the Gibbs free energies of the complex, $C_6H_5OCH_3$, and BF_3 at 298 K and ambient pressure, respectively. We note that the reported values of ΔH and ΔG are not corrected for BSSE.

To understand the binding characteristics of the complexes, we also carried out charge decomposition analysis (CDA).[57,58] The CDA decomposes the wave function (in the case of B3LYP, it is the Kohn−Sham determinant) of the complex in terms of fragment orbitals of the chosen donor A (=$C_6H_5OCH_3$) and acceptor B (=BF_3) in the $C_6H_5OCH_3$−BF_3 1:1 complexes. The charge donation from A to B, q(d), was calculated using the occupied orbitals of A and vacant orbitals of B. The back-donation from B to A, q(b), was calculated using the occupied orbitals of B and vacant orbitals of A. The repulsive polarization term, q(r), was calculated using the occupied orbitals of both fragments, and the residual term, q(s), was calculated using the unoccupied orbitals. Since the basis sets including diffuse functions generate great negative values for the residual term, we used the 6-31G(d,p) basis set in the CDA calculations, a method used by others.[59,60]

3. Results and Discussion

The results obtained for $C_6H_5OCH_3$, BF_3, and their complexes have been summarized in Tables 1−8 and Figures 1−4. In what follows, we will first make comparisons on the structural parameters and energy data obtained by different basis sets and methods and then present and discuss the results for complex formation.

3.1. Comparison of Results from Different Basis Sets and Methods. In this subsection, we compare the effect of basis sets and methods on the results of structural parameters, i.e., bond distance, bond angle, and dihedral angle, as well as binding energies.

The most comprehensive data for such a comparison have been provided in Tables 1−4 for $C_6H_5OCH_3$, BF_3, and their most stable 1:1 complex AB13. The structure of AB13 and the numbering atoms to be discussed below can be found in Figure 1. For the bond distances shown in Table 1, the biggest discrepancy between the 6-31+G(d,p) and 6-311+G(d,p) basis sets is 0.004 Å from the B3LYP calculations and 0.010 Å from the MP2 calculations for monomers, $C_6H_5OCH_3$ or BF_3. However, the discrepancy increases when dealing with the complex AB13. The discrepancy in the distance between O12−B18 increases to 0.016 Å for the B3LYP method and to 0.019 Å for the MP2 method. Furthermore, the O12−B18 distance obtained from MP2 is about 0.040 Å shorter than that from B3LYP. These indicate that a greater difference exists between methods than that between basis sets of the same method. The bond between O12 and B18 is critical in determining how strongly the two monomers bind. Because the MP2 O12−B18 distance is shorter, we expect the MP2 binding energy will be larger than the B3LYP energy. As for the bond angles, the discrepancy in the data, shown in Table 2, is similar to those with the bond distance. The biggest discrepancy occurs in the complex. For instance, the MP2 O12−B18−F19 angle using

TABLE 1: Bond Lengths of BF_3, $C_6H_5OCH_3$, and the Most Stable $C_6H_5OCH_3-BF_3$ 1:1 Complex (AB13)

	$C_6H_5OCH_3$				$C_6H_5OCH_3 \cdot BF_3$			
	B3LYP		MP2		B3LYP		MP2	
bond length (Å)	S[a]	L[a]	S	L	S	L	S	L
r(C1−C2)	1.401	1.398	1.402	1.404	1.398	1.394	1.398	1.400
r(C2−C3)	1.401	1.397	1.400	1.402	1.392	1.388	1.392	1.394
r(C3−C4)	1.404	1.400	1.403	1.405	1.390	1.387	1.390	1.391
r(C4−C5)	1.392	1.388	1.393	1.394	1.397	1.394	1.398	1.400
r(C5−C6)	1.401	1.398	1.401	1.403	1.398	1.394	1.399	1.400
r(C1−C6)	1.394	1.390	1.395	1.396	1.398	1.394	1.399	1.401
r(C3−O12)	1.368	1.366	1.374	1.366	1.420	1.417	1.422	1.414
r(O12−C13)	1.422	1.420	1.426	1.419	1.458	1.456	1.461	1.453
r(C1−H7)	1.087	1.085	1.083	1.087	1.086	1.084	1.083	1.086
r(C2−H8)	1.084	1.082	1.083	1.084	1.084	1.083	1.082	1.085
r(C4−H9)	1.085	1.083	1.083	1.086	1.085	1.083	1.083	1.086
r(C5−H10)	1.086	1.084	1.083	1.087	1.086	1.084	1.083	1.086
r(C6−H11)	1.086	1.084	1.082	1.086	1.086	1.084	1.083	1.086
r(C13−H14)	1.098	1.096	1.092	1.096	1.091	1.089	1.086	1.090
r(C13−H15)	1.098	1.096	1.092	1.096	1.092	1.091	1.087	1.091
r(C13−H16)	1.091	1.089	1.085	1.090	1.088	1.086	1.084	1.088
	BF_3				$C_6H_5OCH_3 \cdot BF_3$			
	B3LYP		MP2		B3LYP		MP2	
bond length (Å)	S[a]	L[a]	S	L	S	L	S	L
r(B18−F17)	1.321	1.317	1.328	1.318	1.363	1.360	1.372	1.360
r(B18−F19)	1.321	1.317	1.328	1.318	1.369	1.365	1.381	1.369
r(B18−F20)	1.321	1.317	1.328	1.318	1.356	1.352	1.366	1.354
r(O12−B18)					1.735	1.751	1.694	1.713

[a] S and L refer to the 6-31+G(d,p) and 6-311+G(d,p) calculations, respectively. The numbered atoms, such as O12, are shown in Figure 1. The structure of the most stable complex AB13 is also shown in Figure 1.

TABLE 2: Bond Angles of $C_6H_5OCH_3$ and the Most Stable $C_6H_5OCH_3-BF_3$ 1:1 Complex (AB13)

	$C_6H_5OCH_3$				$C_6H_5OCH_3 \cdot BF_3$			
	B3LYP		MP2		B3LYP		MP2	
bond angle (deg)	S[a]	L[a]	S	L	S	L	S	L
θ(C1−C2−C3)	119.4	119.5	119.2	119.4	118.3	118.4	117.8	118.1
θ(C2−C3−C4)	119.9	119.8	120.2	119.9	122.5	122.3	123.1	122.8
θ(C3−C4−C5)	112.0	120.0	119.9	120.1	118.6	118.7	118.3	118.4
θ(C4−C5−C6)	120.6	120.6	120.5	120.4	120.2	120.2	120.1	120.1
θ(C5−C6−C1)	119.2	119.2	119.3	119.2	120.1	120.1	120.2	120.2
θ(C6−C1−C2)	121.0	120.9	120.9	120.9	120.4	120.3	120.5	120.4
θ(C2−C3−O12)	124.4	124.5	124.5	124.6	120.1	120.1	120.2	120.2
θ(C4−C3−O12)	115.6	115.7	115.3	115.5	117.4	117.6	116.7	117.0
θ(C3−O12−C13)	118.6	118.6	116.9	116.6	114.8	115.0	113.4	113.2
θ(C3−C2−H8)	121.1	121.1	121.4	121.3	120.3	120.2	120.4	120.3
θ(C1−C2−H8)	119.5	119.5	119.4	119.3	121.4	121.3	121.7	121.6
θ(C2−C1−H7)	119.0	119.0	119.0	118.9	119.5	119.5	119.4	119.4
θ(C6−C1−H7)	120.1	120.0	120.1	120.1	120.2	120.2	120.1	120.1
θ(C1−C6−H11)	120.4	120.4	120.3	120.3	119.9	119.9	119.9	119.9
θ(C5−C6−H11)	120.4	120.4	120.4	120.4	119.9	119.9	119.9	119.9
θ(C6−C5−H10)	120.1	120.0	120.1	120.2	120.2	120.2	120.2	120.2
θ(C4−C5−H10)	119.3	119.4	119.4	119.4	119.6	119.6	119.6	119.6
θ(C5−C4−H9)	121.5	121.4	121.6	121.5	121.7	121.6	122.1	122.1
θ(C3−C4−H9)	118.6	118.5	118.5	118.4	119.7	119.7	119.6	119.5
θ(O12−C13−H14)	111.4	111.5	111.1	111.2	108.0	108.1	107.3	107.6
θ(O12−C13−H15)	111.4	111.5	111.1	111.2	109.8	109.9	109.5	109.7
θ(O12−C13−H16)	105.8	105.8	105.4	105.7	106.0	106.0	105.7	105.9
θ(H14−C13−H15)	109.4	109.4	109.7	109.5	111.0	110.9	111.4	111.0
θ(H14−C13−H16)	109.3	109.3	109.7	109.5	111.0	110.9	111.5	111.0
θ(H15−C13−H16)	109.3	109.3	109.7	109.5	110.8	110.8	111.2	111.2
θ(O12−B18−F19)					103.2	103.2	103.6	103.0
θ(O12−B18−F20)					102.1	102.1	102.3	102.0
θ(F19−B18−F20)					115.8	115.8	115.4	115.6

[a] S and L refer to the 6-31+G(d,p) and 6-311+G(d,p) calculations, respectively. The numbered atoms, such as O12, are shown in Figure 1. The structure of the most stable complex AB13 is also shown in Figure 1.

the 6-31+G(d,p) basis set is 0.6° bigger than that using 6-311+G(d,p). For the same angle, the difference between different methods, i.e., B3LYP and MP2, is 0.4° with the 6-31G+(d,p) basis set and is 0.2° with the 6-311+G(d,p) basis set. Therefore, the discrepancy in predicting bond angles between methods is smaller than that of basis sets. For the dihedral angles, data in Table 3 show that a greater discrepancy exists between methods than between basis sets, which is the

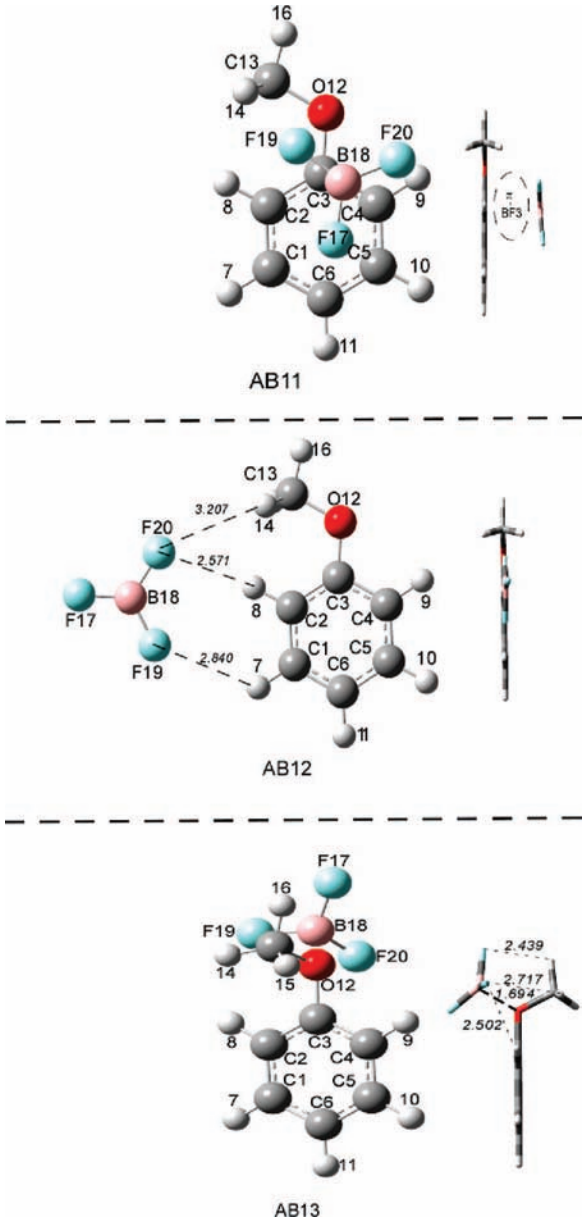

Figure 1. Structures of the $C_6H_5OCH-BF_3$ 1:1 complexes obtained at the MP2/6-31+G(d,p) level.

same in the prediction of bond distances. Despite the above quantitative discrepancies, both methods (MP2 and B3LYP) and basis sets [6-31G+(d,p) and 6-311+G(d,p)] predicted the same structures. As such, any of the methods or basis sets can be used to predict 1:1 complex structures.

We now examine another important issue of the theoretical predictions, i.e., the relative stability of isomers. Table 4 provides the binding energies of three 1:1 complexes that were obtained using different methods and basis sets. Two observations can be made from the comparison of these data. One is that the basis set does not affect the energies much within the same method. However, the binding energies from B3LYP, such as ΔE values in Table 4, are smaller than those from MP2. The second observation is the discrepancy between the methods is not consistent among different complexes. For the complex AB13, the binding energy from MP2 is about three times as big as that from B3LYP. For AB11, the MP2 binding energy is about four times as big, and for AB12, it is about six times. This indicates that the weaker the interaction is in a complex, the greater the discrepancy that exists between the methods.

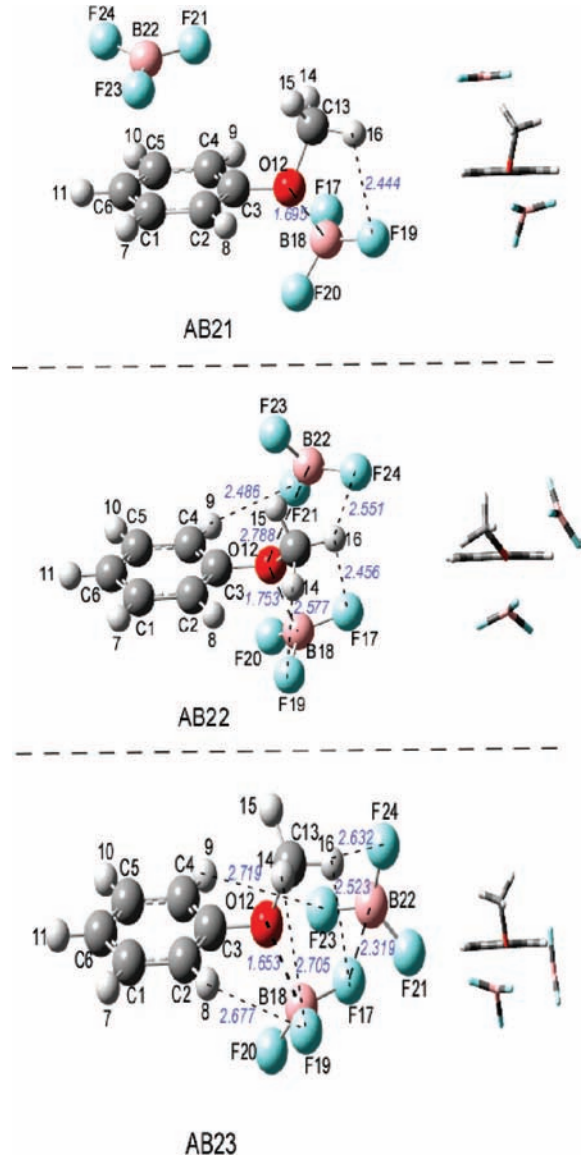

Figure 2. Structures of the $C_6H_5OCH-BF_3$ 1:2 complexes obtained at the MP2/6-31+G(d,p) level.

A comparison was also made between MP2 and B3LYP results using the 6-31+G(d,p) basis set for the 1:2 complexes. The structural data for the most stable 1:2 complex, AB23, are shown in Table 5 with the structure shown in Figure 2. The data in Table 5 show that the biggest discrepancy can be found in the last two distances (B18−B22 and F17−B22), the last two bond angles (O12−B18−F17 and O12−B18−B22), and the last two dihedral angles (F19−B18−C13−H14 and O12−B18−F17−B22). These data describe the moieties of the complex where the three monomers (one $C_6H_5OCH_3$ and two BF_3) interact. This illustrates that the greatest discrepancy occurs in predicting weak interactions. Amid the differences in values, both MP2 and B3LYP predict the same structure. The binding energies shown in Table 6 illustrate that different basis sets give similar results for both MP2 and B3LYP calculations. However, the MP2 binding energies are about three times as large as the B3LYP ones for all three isomers. In addition, there are structures that are stable from B3LYP calculations but are not stable from MP2 calculations. Two of the examples are shown in Figure 3. The structure of complex AB24 was obtained only at the B3LYP/6-31+G(d,p) level; it failed to converge using the 6-311+G(d,p) basis set or the MP2 method. The symmetric

TABLE 3: Dihedral Angles of $C_6H_5OCH_3$ and the Most Stable $C_6H_5OCH_3-BF_3$ 1:1 Complex (AB13)

	$C_6H_5OCH_3$				$C_6H_5OCH_3 \cdot BF_3$			
	B3LYP		MP2		B3LYP		MP2	
dihedral angle (deg)	S[a]	L[a]	S	L	S	L	S	L
ϕ(C1−C2−C3−C4)	0.0	0.0	0.0	1.7	0.4	0.5	0.3	0.4
ϕ(C2−C3−C4−C5)	0.0	0.0	0.0	−1.6	−0.4	−0.5	−0.4	−0.4
ϕ(C3−C4−C5−C6)	0.0	0.0	0.0	1.6	0.1	0.1	0.1	0.1
ϕ(C4−C5−C6−C1)	0.0	0.0	0.0	−1.5	0.3	0.3	0.2	0.3
ϕ(C1−C2−C3−O12)	180.0	180.0	180.0	−179.4	179.8	179.8	179.7	180.0
ϕ(C5−C4−C3−O12)	−180.0	−180.0	−180.0	179.4	−179.9	−179.9	−179.7	−180.0
ϕ(C2−C3−C4−H9)	180.0	180.0	180.0	179.7	178.7	178.6	178.6	178.8
ϕ(C3−C4−C5−H10)	−180.0	−180.0	−180.0	−179.8	179.7	179.7	179.6	179.7
ϕ(C4−C5−C6−H11)	−180.0	−180.0	−180.0	179.9	179.8	179.8	179.7	179.8
ϕ(C5−C6−C1−H7)	−180.0	180.0	180.0	−179.9	179.2	179.2	179.1	179.1
ϕ(C6−C1−C2−H8)	180.0	−180.0	180.0	179.9	178.5	178.4	178.2	178.1
ϕ(C2−C3−O12−C13)	0.0	0.0	0.0	0.4	76.4	76.7	74.5	70.7
ϕ(C4−C3−O12−C13)	−180.0	−180.0	−180.0	179.4	−104.1	−103.9	−106.1	−109.7
ϕ(C3−O12−C13−H14)	61.3	61.3	61.2	61.3	54.0	55.8	54.8	56.0
ϕ(C3−O12−C13−H15)	−61.3	−61.3	−61.2	−61.2	−67.2	−65.4	−66.3	−65.1
ϕ(C3−O12−C13−H16)	180.0	−180.0	180.0	−179.9	173.1	−174.8	173.9	175.1
ϕ(F17−B18−F19−F20)					−140.2	141.2	139.4	140.4
ϕ(C3−O12−C13−B18)					−144.5	−145.9	−137.8	−137.7
ϕ(F19−B18−C13−H14)					7.1	7.6	8.2	9.4
ϕ(B18−O12−C13−H14)					77.3	80.5	71.5	72.7
ϕ(B18−O12−C13−H15)					−161.5	−158.4	−167.4	−166.2
ϕ(B18−O12−C13−H16)					−42.5	−39.4	−48.3	−47.2

[a] S and L refer to the 6-31+G(d,p) and 6-311+G(d,p) calculations, respectively. The numbered atoms, such as O12, are shown in Figure 1. The structure of the most stable complex AB13 is also shown in Figure 1.

TABLE 4: Binding Energies, Formation Enthalpies, and Gibbs Free Energy Changes for the $C_6H_5OCH_3-BF_3$ 1:1 Complexes[a]

	B3LYP						MP2					
	6-31+G(d,p)			6-311+G(d,p)			6-31+G(d,p)			6-311+G(d,p)		
	AB11	AB12	AB13	AB11	AB12	AB13	AB11	AB12	AB13	AB11	AB12	AB13
ΔE	−1.3	−0.3	−5.7	−1.6	−0.3	−5.8	−6.2	−1.8	−14.8	−6.2	−1.9	−13.2
ΔE_{BSSE}	−1.1	−0.2	−4.8	−1.2	−0.2	−4.6	−4.7	−1.4	−11.1	−4.6	−1.4	−9.5
ΔE_0	−0.8	−0.05	−3.9	−1.0	−0.08	−3.7	−3.6	−1.3	−9.3	−3.8	−0.8	−7.8
ΔH_{298}	−0.1	−1.0	−4.6	−0.4	−0.9	−4.7	−4.7	−0.7	−13.2	−4.8	−0.5	−11.7
ΔG_{298}	5.5	2.9	5.7	5.1	2.9	5.4	4.3	3.1	−1.7	3.8	3.8	−0.2

[a] All energies are in kilocalories per mole. ΔE and ΔE_{BSSE} represent the binding energy without and with 50% BSSE correction, respectively. ΔE_0 is the ZPE and 50% BSSE corrected binding energy. The ΔH_{298} and ΔG_{298} represent the formation enthalpies and the Gibbs free energy changes at 298.15 K and ambient pressure. Isomers AB11, AB12, and AB13 differ in the way the BF_3 interacts with anisole in the complex, and their structures are shown in Figure 1.

structure obtained using the B3LYP method, shown as AB25 in Figure 3, cannot be obtained using the MP2 method. Imposing the symmetry of AB25 in the MP2 calculation, we obtained a transition-state structure as it has one imaginary frequency. This illustrates that the B3LYP and MP2 methods may provide very different results including structures when a system includes many monomers and they bind through weak interactions. This is not surprising as the difference in the complex formed by two monomers will magnify further in the complexes formed by more monomers.

As it is well-known that DFT does not describe the weak interactions properly, in the following discussion on the results of complex formation, we will use the data obtained from MP2/6-31+G(d,p) calculations except as otherwise specifically stated.

3.2. $C_6H_5OCH_3-BF_3$ 1:1 Complexes. Since anisole has two prominent proton accepting sites, the lone pair electrons of the oxygen atom and the electron cloud of the aromatic ring, the vacant orbital of boron atom can accept electrons from both sites. As such, we investigated every possible orientation of BF_3 with respect to $C_6H_5OCH_3$ in the 1:1 $C_6H_5OCH_3-BF_3$ complexes and obtained three isomers. The corresponding structures of these isomers are shown in Figure 1. In AB11, the B atom

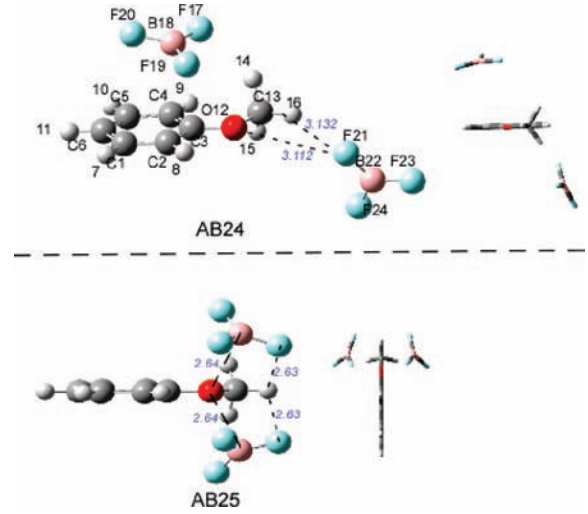

Figure 3. Two structures of the $C_6H_5OCH-BF_3$ 1:2 complexes obtained at the B3LYP/6-31+G(d,p) level.

lies over the aromatic ring, precisely above a C−C bond. This is slightly different from what was predicted in the complex of

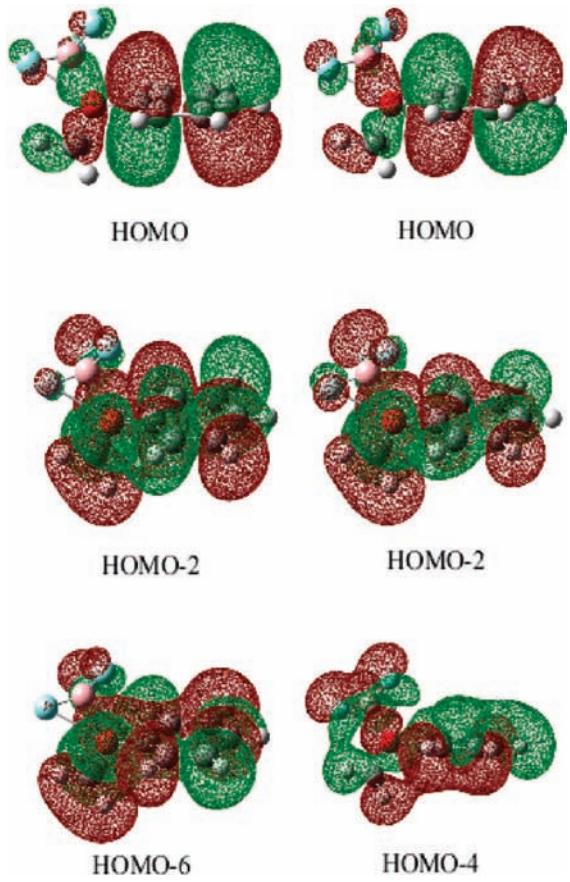

Figure 4. Selected molecular orbitals of the AB13 complex, which is shown in Figure 1. Left pictures were obtained by the MP2/6-31+G(d,p) calculations and the right pictures by the B3LYP/6-31+G(d,p) calculations.

benzene−BF_3. Tarakeshwar et al. studied the interactions between benzene and BF_3, and their results showed that the boron atom lies directly over one of the benzene carbons.[16] Furthermore, our calculated distance between the boron atom and the aromatic ring is 3.015 Å, while it is 2.616 Å in the benzene−BF_3 complex.[16] We attribute this difference to the charge transfer from the aromatic ring to the methoxy group in the anisole−BF_3 complex. In AB12, the BF_3 molecule is almost in the same plane with the aromatic ring and forms the weak H and F bonds, as shown in Figure 1. There are three pairs of interactions: F20 interacts with both H8 (of the aromatic ring) and H14 (of the methyl group) at a distance of 2.571 and 3.207 Å, respectively. F19 interacts with H7 of the aromatic ring, and its distance is 2.840 Å. Since all three distances are significantly longer than the typical hydrogen bond distance of ∼2.0 Å, these interactions are the van der Waals interactions.

As shown in the right pictures of Figure 1, the most striking difference between AB13 and AB11 or AB12 is that the methoxy group is out of the plane of benzene ring with a dihedral angle of 74.5°. The planar conformation of the methoxy group and the benzene ring is the most stable for the anisole monomer and also in AB11 and AB12. The study of anisole−ammonia complexes by Piani et al. showed that the planar conformation of anisole remains in the complexes.[25] In the work of Reimann et al.[22] and Becucci et al.,[23] both results showed that the planar conformation of anisole still remains in the anisole−water 1:1 complexes, where the water molecule forms the hydrogen bond with the oxygen atom of anisole with its center of mass lying above the aromatic ring. We note that the rotation barrier of the methoxy group in anisole was found to be about 3 kcal/mol by different groups.[19,20,61−63] Additionally, our calculated B−O distance in AB13 is 1.713 Å at the MP2/6-311+G(d,p) level this is longer than that in the 1:1 complexes of BF_3 interacting with dimethyl ether, diethyl ether, ethylene oxide, and methanol, in which the B−O distances are 1.671, 1.642, 1.705, and 1.687 Å (obtained at the MP2/6-311++G(3df,2pd) level), respectively.[24] For AB13, there are also three pairs of additional H−F interactions; i.e., F17 interacts with H16 with the shortest distance of 2.439 Å on one side of the C3−O12−C13 plane and F19 interacts with both H8 and H14 on the opposite side with the distance of 2.507 and 2.717 Å, respectively. Due to these interactions, a huge pyramidalization occurs in BF_3 molecule with a F17−B18−F19−F20 dihedral angle of 139.4°. Thus both the B−O and F−H interactions are responsible for the structural differences of AB13 with respect to those of isomers AB11 and AB12. We mention that both B−O and F−H interactions were also found in the complexes of BF_3 with CH_3OH, CH_3COOH, $(CH_3)_2O$, $(CH_3CH_2)_2O$, and $(CH_2)_2O$.[24]

The existence of a strong donor−acceptor interaction between B and O in AB13, in comparison with the other two isomers, indicates that AB13 may be the most stable isomer of all. The calculated binding energies for these 1:1 complexes are shown in Table 4. Isomer AB13 has a binding energy of −9.3 kcal/mol and is indeed the most stable isomer.

Our calculated binding energy, ΔE_0, for the isomer AB11 is −3.6 kcal/mol. This is slightly bigger than that of the benzene−BF_3 complex, which has a binding energy of −2.44 kcal/mol.[16] Thus, it implies the attached methoxy group can enhance the nucleophilicity of the benzene ring. In the case of isomer AB12, BF_3 interacts with the hydrogen atom of anisole through weak F−H interaction. The binding energy of AB12 is −1.3 kcal/mol, which is much smaller than those of AB11 and AB13. This again indicates that the oxygen atom dominates the proton affinity of anisole and the benzene ring generally compensates the nucleophilicity of oxygen. Thus, the relative proton affinities in anisole are in the order of oxygen atom > aromatic ring > methyl group. This is consistent with the study on the protonation and proton affinity of anisole, which showed that the methoxy group has a strong influence on the protonation of anisole with respect to the aromatic ring.[21]

The isomer structures shown in Figure 1 illustrate clearly that anisole molecule interacts with BF_3 in three styles: O−B, π−B, and H−F. To gain insight into the nature of the interactions in the $C_6H_5OCH_3$−BF_3 complexes, we performed charge decomposition analysis (CDA).[57,58] Table 7 summarizes the total amounts of donation, q(d)($C_6H_5OCH_3 \rightarrow BF_3$), back-donation, q(b)($C_6H_5OCH_3 \leftarrow BF_3$), repulsion, q(r)($C_6H_5OCH_3 \leftrightarrow BF_3$), and residual term, q(s), for the three $C_6H_5OCH_3$−BF_3 1:1 complexes. As the data in Table 7 shows, the B3LYP and MP2 results agree generally well.

As the data shows in Table 7, there is a significant increase in the amount of $C_6H_5OCH_3 \rightarrow BF_3$ donation from AB11 to AB13, both of which are electrophilic processes as $q(d)/q(b) = 1.27$ for AB11 and $q(d)/q(b) = 4.80$ for AB13 (obtained using the MP2 method). The q(d) values confirm that the donation from the oxygen lone pair electrons to the vacant orbital of boron atom is significantly larger than the $\pi \rightarrow BF_3$ donation. There is also a large back-donation in AB13, which occurs by the electron transfer from the lone pair electrons of fluorine atom to the vacant orbitals of hydrogen atoms of anisole. There are no significant donation and back-donation in AB12, which means that the F−H interaction is the weakest interaction among the three types of interactions. However, in AB12 the back-

TABLE 5: Bond Lengths (r, Å), Bond Angles (θ, deg), and Dihedral angles (ϕ, deg) of the Most Stable $C_6H_5OCH_3-BF_3$ 1:2 Complex (AB23) Obtained Using the 6-31+G(d, p) Basis Set[a]

	B3LYP	MP2		B3LYP	MP2
			Bond Lengths		
r(C2−C3)	1.391	1.391	r(C13−H15)	1.088	1.087
r(C3−C4)	1.389	1.389	r(C13−H16)	1.090	1.084
r(C3−O12)	1.424	1.425	r(B18−F17)	1.384	1.396
r(O12−C13)	1.463	1.465	r(B18−F19)	1.368	1.376
r(C2−H8)	1.085	1.082	r(O12−B18)	1.685	1.653
r(C4−H9)	1.085	1.082	r(B18−B22)	3.539	3.288
r(C13−H14)	1.091	1.086	r(F17−B22)	2.441	2.319
			Bond Angles		
θ(C1−C2−C3)	118.2	117.7	θ(O12−C13−H14)	109.5	109.2
θ(C2−C3−C4)	122.8	123.5	θ(O12−C13−H16)	106.2	105.9
θ(C3−C4−C5)	118.4	117.9	θ(H14−C13−H16)	111.2	111.5
θ(C2−C3−O12)	119.9	119.8	θ(O12−B18−F19)	104.5	104.9
θ(C4−C3−O12)	117.3	116.8	θ(O12−B18−F17)	101.6	101.4
θ(C3−O12−C13)	114.8	113.5	θ(O12−B18−B22)	82.9	75.2
θ(C3−C2−H8)	120.4	120.5	θ(B18−F17−B22)	133.5	122.6
			Dihedral Angles		
ϕ(C1−C2−C3−C4)	−0.5	−0.3	ϕ(C3−O12−C13−H14)	67.3	63.9
ϕ(C2−C3−C4−C5)	0.5	0.4	ϕ(C3−O12−C13−H16)	−172.6	−176.0
ϕ(C3−C4−C5−C6)	−0.2	0.0	ϕ(F17−B18−F19−F20)	−136.1	−135.4
ϕ(C1−C2−C3−O12)	−180.0	−180.0	ϕ(B18−O12−C13−H14)	−77.8	−75.6
ϕ(C5−C4−C3−O12)	−180.0	−180.0	ϕ(B18−O12−C13−H16)	42.3	44.5
ϕ(C6−C1−C2−H8)	−178.5	−178.3	ϕ(F21−B22−F23−F24)	−171.7	−169.6
ϕ(C2−C3−O12−C13)	−76.8	−74.9	ϕ(F19−B18−C13−H14)	−13.5	−20.4
ϕ(C4−C3−O12−C13)	103.7	105.4	ϕ(O12−B18−F17−B22)	−52.6	−44.7

[a] The numbering atoms, such as O12, are shown in Figure 2. The structure of the most stable complex AB23 is also shown in Figure 2.

donation slightly dominates the charge transfer as $q(d)/q(b) < 1$. The relative values shown in Table 7 showed that the charge transfer is the order of AB13 ≫ AB11 > AB12, which agrees well with the binding energy analysis, in which the order of stability is AB13 > AB11 > AB12. Finally, we note that the depleted charge from the overlapping area of the occupied orbitals is expressed by the negative values of the repulsion term $q(r)$.

To further analyze and compare the donor−acceptor relationship, we plotted three molecular orbitals of AB13 in Figure 4. The CDA results showed that three molecular orbitals (MOs), HOMO, HOMO-2, and HOMO-6, dominate the donation, in which the electron donation amount is 0.008, 0.027, and 0.054, respectively. The left pictures of Figure 4 are these three MOs from MP2 calculations and it is clear that, in each case, there is a strong donation from the lone pair electrons of the oxygen atom to the vacant p orbital of the boron atom. Further analysis showed that these orbitals, i.e., HOMO, HOMO-2, and HOMO-6, of AB13 are the overlap between LUMO+4 of BF_3 and HOMO, HOMO-3, and HOMO-4 of anisole, respectively. The MOs from B3LYP calculations are not entirely the same as those of the MP2 method. The comparison of MOs in Figure 4 shows that, among the three B3LYP MOs, the HOMO (its contribution to $q(d)$ is 0.017) and HOMO-2 (0.042) of AB13 are similar to the corresponding MP2 MOs, but the third significant overlap B3LYP orbital is HOMO-4 (0.033) and there is no overlap in HOMO-6.

3.3. $C_6H_5OCH_3-BF_3$ 1:2 Complexes. Reimann et al. investigated the interaction of anisole with two water molecules and found that the addition of a single water molecule to the 1:1 complexes can result in the emergence of a strong and competitive σ-H interaction.[22] Furthermore, Dehaan et al.'s work showed a fluorine bridge between boron atoms in the benzene−BF_3 1:2 complexes.[64] These studies suggest that it may be possible that anisole will bind with more than one BF_3 molecules. As such, we studied how strongly the anisole−BF_3 1:2 complexes bind. Since there are three main binding sites in anisole, i.e., oxygen atom, aromatic ring, and methyl group, we calculated several complexes in which the BF_3 molecules were initially located at various places with respect to the anisole. The calculations, however, mainly converged into three isomers, AB21, AB22, and AB23, which are shown in Figure 2. As shown in Figure 2, in AB21, one BF_3 interacts with the oxygen atom with a BO distance of 1.695 Å and the other BF_3 interacts with the aromatic ring. Further, the BF_3 that interacts with the oxygen atom has a pyramidal structure. The rotation of anisole is 77.2°. In AB22, both BF_3 molecules interact with the oxygen atom of anisole, and the B−O distances are 1.753 and 2.788 Å, respectively, which are significantly longer than that in AB21 (1.695 Å). The rotation of anisole in AB22 is 42.1°. Also, the BF_3 that is closer to the oxygen atom has an obvious pyramidal structure.

In AB23, the B−O distance is 1.653 Å, which is the shortest, compared to those in AB21 and AB22. The additional BF_3 interacts with the fluorine atom (F17) of the first BF_3, as shown in Figure 2. Specifically, the boron atom of the additional BF_3 interacts with the lone pair electrons of F17, receiving electrons from the fluorine atom and forming a fluorine bridge between the boron atoms. The same fluorine bridge was also observed in the benzene−$(BF_3)_2$ complexes.[64] Thus, there is an additional FB σ bond with a distance of 2.319 Å in AB23, compared to that in AB13. The visible pyramidal structure can be found in the BF_3 molecule that interacts with the oxygen atom. Finally note that the rotation of anisole in AB23 is 105.4°.

In summary, in all $C_6H_5OCH_3-BF_3$ 1:2 complexes, one BF_3 molecule interacts with the oxygen atom through a Lewis acid−base donor−acceptor interaction, which forms the structure very similar to AB13, and the other BF_3 interacts with the aromatic ring (AB21), the oxygen atom (AB22), or the fluorine atom (AB23) through three different interactions: π-BF_3, O−B, and F−B.

TABLE 6: Binding Energies, Formation Enthalpies, and Gibbs Free Energy Changes for the 1:2 $C_6H_5OCH_3-BF_3$ Complexes Obtained Using the 6-31+G(d, p) Basis Set[a]

	B3LYP			MP2		
	AB21	AB22	AB23	AB21	AB22	AB23
ΔE	−6.8	−6.4	−9.5	−20.1	−19.8	−23.0
ΔE_{BSSE}	−6.6	−5.9	−9.1	−18.7	−18.2	−21.4
ΔE_0	−5.4	−4.5	−7.7	−16.4	−15.7	−18.9
ΔH_{298}	−4.5	−3.8	−7.3	−17.3	−17.0	−20.3
ΔG_{298}	11.2	13.0	11.1	2.0	3.0	0.7

[a] All energies are in kilocalories per mole. ΔE and ΔE_{BSSE} represent the binding energy without and with 50% BSSE correction, respectively. ΔE_0 is the ZPE and 50% BSSE corrected binding energy. The ΔH_{298} and ΔG_{298} represent the formation enthalpies and the Gibbs free energy changes at 298.15 K and ambient pressure. The structures of AB21, AB22, and AB23 are shown in Figure 2.

TABLE 7: Charge Decomposition Analysis (CDA) of $C_6H_5OCH_3-BF_3$ Complexes Obtained Using the B3LYP and MP2 with the 6-31G(d,p) Basis Set[a]

	q(d)	q(b)	q(r)	q(s)
		B3LYP		
AB11	0.031	0.011	−0.006	0.000
AB12	0.002	0.017	−0.001	0.000
AB13	0.283	0.058	−0.267	0.001
		MP2		
AB11	0.033	0.026	−0.024	−0.001
AB12	0.001	0.028	−0.005	−0.000
AB13	0.235	0.049	−0.232	−0.004

[a] In CDA the anisole→BF_3 donation, q(d), was calculated by examining the occupied orbitals of anisole and vacant orbitals of BF_3. The BF_3→anisole back-donation, q(b), was calculated by examining the occupied orbitals of BF_3 and vacant orbitals of anisole. The repulsive polarization term, q(r), was obtained through analysis of the occupied orbitals of both fragments, and the residual term, q(s), by the unoccupied orbitals.

Comparing the structural parameters of the anisole monomer with the most stable 1:1 and 1:2 complexes (AB13 and AB23), we found that the C3−O12 distance of anisole increases from 1.374 to 1.422 to 1.425 Å from the anisole monomer to the 1:1 and to the 1:2 complex, respectively. Similarly, the O12−C13 distance increases from 1.426 to 1.453 to 1.465 Å, respectively. These can be explained by the increasing charge transfer from the oxygen lone pair electrons to the vacant orbital of B18 from the monomer to the 1:1 to the 1:2 complex. There are slight decreases for C2−H8, C13−H14, and C13−H16 distances due to the electron donation from the fluorine atoms to the hydrogen atoms (F19 to both H8 and H14, and F17 to H16). Additionally, there is a large rotation of the methoxy group (from 0.0 in anisole monomer to 74.5° in AB13 and to 105.4° in AB23). The BF_3 molecule in AB13 has a pyramidal structure with a F17−B18−F19−F20 dihedral angle of 139.4°. In AB23, the second BF_3 molecule tends to flatten this F17−B18−F19−F20 pyramidalization angle from 139.4 to 135.4° because of the F17−B22 interaction. Furthermore, the second BF_3 itself has a small F21−B22−F23−F24 dihedral angle of −169.6°.

The energetics of three 1:2 complexes are summarized in Table 6. The calculated binding energy (ΔE_0) of AB23 complex is −18.9 kcal/mol, which is the largest compared to those of AB21 (−16.4 kcal/mol) and AB22 (−15.7 kcal/mol). The structural difference between AB23 and the other two isomers (AB21 and AB22) is that the two BF_3 molecules in AB23 interact with each other through the F and B atom, while, in AB21, the second BF_3 molecule acts as a Lewis acid to the aromatic ring, and in AB22, both BF_3 molecules interact with oxygen atom. This indicates that the BF_3-BF_3 interaction is stronger than the other interactions.

TABLE 8: Charge Decomposition Analysis (CDA) Obtained at the B3LYP and MP2 Levels for C_6H_5OCH-BF_3 1:2 Complexes[a]

	q(d)	q(b)	q(r)	q(s)
		B3LYP		
AB21	0.029	0.014	−0.006	−0.000
AB22	0.063	0.044	−0.028	−0.002
AB23	0.100	0.030	−0.020	0.004
		MP2		
AB21	0.038	0.026	−0.020	−0.001
AB22	0.020	0.050	−0.023	−0.002
AB23	0.080	0.040	−0.027	−0.002

[a] In CDA the $C_6H_5OCH_3-BF_3$→BF_3 donation, q(d), is given by evaluating the occupied orbitals of $C_6H_5OCH_3\cdot BF_3$ and vacant orbitals of BF_3. The BF_3→$C_6H_5OCH_3\cdot BF_3$ back-donation, q(b), is given by evaluating the occupied orbitals of BF_3 and vacant orbitals of $C_6H_5OCH_3\cdot BF_3$. The analysis of the occupied orbitals of both fragments gives the repulsive polarization term q(r), and the analysis of the unoccupied orbitals gives the residual term q(s).

As in all 1:2 complexes, one of the BF_3 molecules interacts with the oxygen atom while the other interacts with the aromatic ring, the oxygen atom, or the first BF_3; we defined the moiety between anisole and the first BF_3 molecule that interacts with the oxygen atom as the electron donor and the second BF_3 molecule as the acceptor in the CDA. The CDA results are shown in Table 8. In the case of AB21, the donation from the aromatic ring to the additional BF_3 molecule is 0.038, which is very close to the donation in AB11 (0.033). The largest donation among 1:2 complexes occurs in AB23, in which the electrons are donated from the lone pair of the fluorine atom (F17) to the vacant orbital of the boron atom (B22). Note that the donation discussed here is much smaller than those in AB13, which means the F−B interaction is much weaker than the O−B interaction. In AB22, the back-donation is 0.050 and the donation is 0.020. It illustrates that the back-donation dominates the electron transfer in the F−H interactions. Although the second BF_3 also interacts with the oxygen atom, the donation is the smallest among all three complexes in Table 8. This is due to the long distance between the oxygen and boron atoms (2.788 Å) in comparison with the O12−B18 distance of 1.753 Å.

Finally, to predict the ratio of anisole to boron trifluoride in the complexes, it is necessary to compare the binding energies of the 1:1 and 1:2 complexes with the experimental measurement. The calculated binding energy of AB13 is in the range of −9.3 to −13.0 kcal/mol (note that −13.0 kcal/mol was obtained including only the ZPE correction but without the 50% BSSE correction). This value is close to the experimental heat of formation measured for the anisole−BF_3 complex (−12.1 ± 0.1 kcal/mol).[5] On the other hand, the calculated binding energy for the 1:2 complexes is −18.9 kcal/mol. Thus, we conclude that the 1:1 complexes with AB13 structure exist most likely in the anisole and BF_3 mixture. The Gibbs free energy changes shown in Table 4 and Table 6 also showed that the formation of AB13 is the only spontaneous reaction at room temperature, which further supports the above conclusion. Although at room temperature the complexes formed as the Lewis acid−base adduct, AB13, most likely exist, we expect that the van der Waals complexes, such as AB11 and AB12, will exist at lower temperatures as well.

4. Conclusions

The complex formation between $C_6H_5OCH_3$ and BF_3 was studied using MP2 and B3LYP methods with 6−31+G(d,p) and 6−311+G(d,p) basis sets. The results show that both B3LYP and MP2 methods predict the same structures and relative stability of $C_6H_5OCH_3-BF_3$ 1:1 isomers; however, the B3LYP binding energies are smaller than the MP2 energies. The discrepancy increases when the interaction becomes weaker. Among the 1:1 complexes, the CDA results indicate that the complexes can be classified as the Lewis acid−base adduct or the van der Waals complexes. There is a significant donation from the oxygen lone pair electrons to the boron vacant orbital in the Lewis acid−base adduct. The interactions among the van der Waals complexes are between the aromatic ring and BF_3 or between the H and F atoms. The MP2 results predict that the adduct formation at room temperature is thermodynamically favorable. Among the 1:2 complexes, the most stable structure consists of both the Lewis acid−base and van der Waals binding; i.e., one BF_3 binds with anisole to form $C_6H_5OCH_3 \cdot BF_3$ adduct, while the other BF_3 binds with this adduct through the van der Waals interactions. From the comparison between the calculated binding energies and the experimental measurement of the heat of formation, we conclude that the 1:1 complexes are the most likely species in the $C_6H_5OCH_3$ and BF_3 mixture. At room temperature, the Lewis acid−base adduct is the structure of the complexes.

Acknowledgment. We are grateful to the support from the Tianjin Science and Technology Project, China (Grant 07ZCKFGX03900) and the NSF (Grant CBET-0709113). The fellowship from the China Scholarship Council is awarded to T.L. for his visit to the Southern Illinois University Carbondale.

Supporting Information Available: Frequencies for all the complexes reported. This information is available free of charge via the Internet at http://pubs.acs.org.

References and Notes

(1) Zuttel, A.; Borgschulte, A.; Orimo, S.-I. *Scr. Mater.* **2007**, *56*, 823.
(2) Ge, Q. *J. Phys. Chem. A* **2004**, *108*, 8682.
(3) Zarkevich, N. A.; Johnson, D. D. *Phys. Rev. Lett.* **2008**, *100*, 040602.
(4) Lewis, F. D.; Barancyk, S. V. *J. Am. Chem. Soc.* **1989**, *111*, 8653.
(5) Palko, A. A.; Healy, R. M.; Landau, L. *J. Chem. Phys.* **1958**, *28*, 214.
(6) Han, L.; Yu, J.; Wang, H.; Lin, T.; Zhang, W. *Proc. Int. Forum Green Chem. Sci. Eng. Process Syst. Eng.* **2006**, *3*, 1735.
(7) Wei, F.; Zhang, W.; Han, M.; Han, L.; Zhang, X.; Zhang, S. *Chem. Eng. Process.* **2008**, *47*, 17.
(8) Palko, A. A.; Begun, G. M.; Landan, L. *J. Chem. Phys.* **1962**, *37*, 552.
(9) Palko, A. A.; Drury, J. S. *J. Chem. Phys.* **1967**, *46*, 2297.
(10) Taillandier, E.; Taillandier, M. *Compt. Rend. Ser. C* **1966**, *263*, 1265.
(11) Wirth, H. E.; Jackson, M. J.; Griffiths, H. W. *J. Phys. Chem.* **1958**, *62*, 871.
(12) Herrebout, W. A.; Lundell, J.; van der Veken, B. J. *J. Phys. Chem. A* **1999**, *103*, 7639.
(13) Herrebout, W. A.; van der Veken, B. J. *Phys. Chem. Chem. Phys.* **1999**, *1*, 3445.
(14) Herrebout, W. A.; Szostak, R.; van der Veken, B. J. *J. Phys. Chem. A* **2000**, *104*, 8480.
(15) Stolov, A. A.; Herrebout, W. A.; van der Veken, B. J. *J. Am. Chem. Soc.* **1998**, *120*, 7310.
(16) Tarakeshwar, P.; Lee, S. J.; Lee, J. Y.; Kim, K. S. *J. Phys. Chem. B* **1999**, *103*, 184.
(17) Van der Veken, B. J.; Sluyts, E. J. *J. Phys. Chem. A* **1997**, *101*, 9070.
(18) Herrebout, W. A.; Lundell, J.; van der Veken, B. J. *J. Phys. Chem. A* **1998**, *102*, 10173.
(19) Spellmeyer, D. C.; Grootenhuis, P. D. J.; Miller, M. D.; Kuyper, L. F.; Kollman, P. A. *J. Phys. Chem.* **1990**, *94*, 4483.
(20) Tsuzuki, S.; Houjou, H.; Nagawa, Y.; Hiratani, K. *J. Phys. Chem. A* **2000**, *104*, 1332.
(21) Catalan, J.; Yanez, M. *J. Am. Chem. Soc.* **1979**, *101*, 3490.
(22) Reimann, B.; Buchhold, K.; Barth, H. D.; Brutschy, B.; Tarakeshwar, P.; Kim, K. S. *J. Chem. Phys.* **2002**, *117*, 8805.
(23) Becucci, M.; Pietraperzia, G.; Pasquini, M.; Piani, G.; Zoppi, A.; Chelli, R.; Castellucci, E.; Demtroeder, W. *J. Chem. Phys.* **2004**, *120*, 5601.
(24) Saenz, P.; Cachau, R. E.; Seoane, G.; Kieninger, M.; Ventura, O. N. *J. Phys. Chem. A* **2006**, *110*, 11734.
(25) Piani, G.; Pasquini, M.; Pietraperzia, G.; Becucci, M.; Armentano, A.; Castellucci, E. *Chem. Phys. Lett.* **2007**, *434*, 25.
(26) Legon, A. C.; Warner, H. E. *J. Chem. Soc., Chem. Commun.* **1991**, 1397.
(27) Hankinson, D. J.; Almlof, J.; Leopold, K. R. *J. Phys. Chem.* **1996**, *100*, 6904.
(28) Nxumalo, L. M.; Andrzejak, M.; Ford, T. A. *Vib. Spectrosc.* **1996**, *12*, 221.
(29) Ghosh, D. C.; Bhattacharyya, S. *Int. J. Mol. Sci* **2004**, *5*, 239.
(30) Herbst, R. S.; Mcsandlerss, S. P. *Sep. Sci. Technol.* **1994**, *29*, 1293.
(31) Bachman, G. B.; Feuer, H.; Bluestein, B. R.; Vogt, C. M. *J. Am. Chem. Soc.* **1955**, *77*, 6188.
(32) Reeve, S. W.; Burns, W. A.; Lovas, F. J.; Suenram, R. D.; Leopold, K. R. *J. Phys. Chem.* **1993**, *97*, 10630.
(33) Nxumalo, L. M.; Andrzejak, M.; Ford, T. A. *J. Chem. Inf. Comput. Sci.* **1996**, *36*, 377.
(34) Hillier, I. H.; Vincent, M. A.; Connor, J. A.; Guest, M. F.; Macdowell, A. A.; Vonniessen, W. *J. Chem. Soc., Faraday Trans.* **1988**, *84*, 409.
(35) Pradeep, T.; Sreekanth, C. S.; Hegde, M. S.; Rao, C. N. R. *J. Am. Chem. Soc.* **1989**, *111*, 5058.
(36) Laszlo, P.; Teston, M. *J. Am. Chem. Soc.* **1990**, *112*, 8750.
(37) Branchadell, V.; Oliva, A. *J. Am. Chem. Soc.* **1991**, *113*, 4132.
(38) Palko, A. A. *J. Chem. Phys.* **1959**, *30*, 1187.
(39) Palko, A. A.; Drury, J. S. *J. Chem. Phys.* **1960**, *33*, 779.
(40) Biczysko, M.; Piani, G.; Pasquini, M.; Schiccheri, N.; Pietraperzia, G.; Becucci, M.; Pavone, M.; Barone, V. *J. Chem. Phys.* **2007**, *127*, 144303.
(41) Frisch, M. J.; Trucks, G. W.; Schlegel, H. N.; Scuseria, G. E.; Robb, M. A.; Cheeseman, J. R.; Montgomery, J. A. J.; Vreven, T.; Kudin, K. N.; Burant, J. C.; Millam, J. M.; Iyengar, S. S.; Tomasi, J.; Barone, V.; Mennucci, B.; Cossi, M.; Scalamni,G.; Rega, N.; Petersson, G. A.; Nakatsuji, H.; Hada, M.; Ehara, M.; Toyota, K.; Fukuda, R.; Hasegawa, J.; Ishida, M.; Nakajima, T.; Honda, Y.; Kitao, O.; Nakai, H.; Klene, M.; Li, X.; Knox, J. E.; Hratchian, H. P.; Cross, J. B.; Bakken, V.; Adamo, C.; Jaramillo, J.; Gomperts, R.; Stramann, R. E.; Yazyev, O.; Austin, A. J. ; Cammi, R.; Pomelli, C.; Ochterski, J. W.; Ayala, P. Y. ; Morokuma, K.; Voth, G. A.; Salvador, P.; Dannenberg, J. J.; Zakrzewski, V. G.; Dapprich, S.; Daniels, A. D.; Strain, M. C.; Farkas, O.; Malick, D. K.; Rabuck, A. G.; Clifford, S.; Cioslowski, J.; Stefanov, B. B.; Liu, G.; Liashenko, A.; Piskorz, P.; Komaromi, I.; Martin, R. L.; Fox, D.J.; Keith, T.; Al-Laham, M. A.; Peng, C. Y.; Nanayakkara, A.; Challacombe, M.; Grill, P. M. W.; Johnson, B.; Chen, W.; Wong, M. W.; Gonzalez, C.; Pople, J. A. *Gaussian 03*, Revision B.05; Gaussian, Inc.: Wallingford, CT, 2004.
(42) Møller, C.; Plesset, M. S. *Phys. Rev.* **1934**, *46*, 618.
(43) Frisch, M. J.; Headgordon, M.; Pople, J. A. *Chem. Phys. Lett.* **1990**, *166*, 275.
(44) Becke, A. D. *J. Chem. Phys.* **1993**, *98*, 5648.
(45) Becke, A. D. *Phys. Rev. A* **1998**, *38*, 3098.
(46) Lee, C.; Yang, W.; Parr, R. G. *Phys. Rev. B* **1998**, *37*, 785.
(47) Miehlich, B.; Savin, A.; Stoll, H.; Preuss, H. *Chem. Phys. Lett.* **1989**, *157*, 200.
(48) Boys, S. F.; Bernardi, F. *Mol. Phys.* **1970**, *19*, 553.
(49) Kim, K. S.; Parakeshwar, P.; Lee, J. Y. *Chem. Rev.* **2000**, *100*, 4145.
(50) Tarakeshwar, P.; Choi, H. S.; Lee, S. J.; Lee, J. Y.; Kim, K. S.; Ha, T. K.; Jang, J. H.; Lee, J. G.; Lee, H. *J. Chem. Phys.* **1999**, *111*, 5838.
(51) Tarakeshwar, P.; Kim, K. S.; Brutschy, B. *J. Chem. Phys.* **1999**, *110*, 8501.
(52) Lee, J. Y.; Kim, J.; Lee, H. M.; Tarakeshwar, P.; Kim, K. S. *J. Chem. Phys.* **2000**, *113*, 6160.
(53) Tarakeshwar, P.; Kim, K. S.; Brutschy, B. *J. Chem. Phys.* **2000**, *112*, 1769.
(54) Tarakeshwar, P.; Kim, K. S.; Brutschy, B. *J. Chem. Phys.* **2001**, *114*, 1295.
(55) Tarakeshwar, P.; Kim, K. S.; Djafari, S.; Buchhold, K.; Reimann, B.; Barth, H. D.; Brutschy, B. *J. Chem. Phys.* **2001**, *114*, 4016.
(56) Kim, K. S.; Lee, J. Y.; Choi, H. S.; Kim, J. S.; Jang, J. H. *Chem. Phys. Lett.* **1997**, *265*, 497.
(57) Dapprich, S.; Frenking, G. *J. Phys. Chem.* **1995**, *99*, 9352.
(58) Frenking, G.; Pidun, U. *J. Chem. Soc., Dalton Trans.* **1997**, 1653.
(59) Decker, S. A.; Klobukowski, M. *J. Am. Chem. Soc.* **1998**, *120*, 9342.
(60) Georgieva, I.; Trendafilova, N. *J. Phys. Chem. A* **2007**, *111*, 13075.
(61) Schaefer, T.; Penner, G. H. *J. Mol. Struct.* **1987**, *157*, 179.
(62) Schaefer, T.; Penner, G.H.]?> *Can. J. Chem.* **1988**, *66*, 1635.
(63) Schaefer, T.; Sebastian, R. *Can. J. Chem.* **1989**, *67*, 1148.
(64) Dehaan, F. P.; Chan, W. H.; Chen, W. D.; Ferrara, D. M.; Giggy, C. L.; Pinkerton, M. J. *J. Org. Chem.* **1989**, *54*, 1206.

JP805748B